NONLINEAR STOCHASTIC DYNAMIC ANALYSIS OF SEISMICALLY ISOLATED STRUCTURES USING TAIL-EQUIVALENT LINEARIZATION METHOD

Ziqi Wang[(1)], Zhishan Li[(2)], Marco Broccardo[(3)]

[(1)] *Assistant Researcher, Earthquake Engineering Research & Test Center, Guangzhou University, ziqidwang@yahoo.com*
[(2)] *Professor, Earthquake Engineering Research & Test Center, Guangzhou University, lizhishan@gzhu.edu.cn*
[(3)] *Postdoc Researcher, Structural Dynamics & Earthquake Engineering research group, ETH Zürich, broccardo@ibk.baug.ethz.ch*

Abstract

This study investigates the application of the tail-equivalent linearization method (TELM) to nonlinear stochastic dynamic analysis of seismically isolated structures. For general multi-degree-of-freedom structural systems, with the ground motion discretized by a finite set of random variables, TELM can be used to compute probability distributions of nonlinear responses as well as seismic fragility functions. The tail-equivalent linear system (TELS) is an equivalent system in the sense that the failure probability of TELS is identical to the first-order approximation of the failure probability of the nonlinear system, and TELS is numerically defined by a discretized impulse-response function or frequency-response function. A typical building model with seismic isolation bearing and a corresponding non-isolated model are used to study the influence of seismic isolation on the seismic reliability of the structure. Two stochastic ground motion models corresponding to different soil conditions are considered to investigate the influence of soil condition on the effectiveness of seismic isolation.

Keywords: Nonlinear analysis; Random vibration; Seismic isolation; Stochastic dynamics; Tail-equivalent linearization;

1. Introduction

In the past few decades, seismic isolation has become one of the most effective techniques to improve the seismic performance of structures. In seismic isolated structures, the structural fundamental period is split in a longer period (bearing period) and shorter period (superstructure period); moreover, the energy dissipating capacity of the structure can be increased by using specific dissipators. Consequently, the seismic effect on the superstructure can be largely reduced. Nonlinear analysis is often required to investigate the performance of seismically isolated structures because most of the seismic isolators are characterized by inelastic constitutive laws. Moreover, considering the intrinsic stochastic nature of ground motions, it is of interest to use nonlinear stochastic dynamic analysis to study the seismic performance of seismically isolated structures.

The equivalent linearization method (ELM) [1-4] is one of the most widely-used approaches for nonlinear stochastic dynamic analysis of multi-degree-of-freedom (MDOF) systems, and it has been employed in several applications involving base-isolated structures [5-8]. In general, the conventional ELM is accurate in estimating mean-square responses; however, estimations of crossing rates, first-passage probability and fragility functions can be far from correct [9].

A recent alternative to ELM is the tail-equivalent linearization method (TELM) [9,10]. Similar to the conventional ELM, TELM is applicable to general MDOF structural systems; however, TELM has superior accuracy in estimating crossing rates, first-passage probability, and fragility functions particularly in the tail region. Moreover, in contrast to the conventional ELM, TELM is a non-parametric method in the sense that there is no need to select a parametric linear system. The tail-equivalent linear system (TELS) is numerically obtained in terms of a discretized impulse-response function (IRF) or frequency-response function (FRF), thus allowing more flexibility in the linearization.

The time- and frequency-domain TELMs have been applied to various problems with *non-isolated* structural systems [9-13]. However, to our knowledge, the application of TELM to structures with base isolation has not been fully investigated. Motivated by the aforementioned perspective, this paper illustrates TELM for application to the nonlinear stochastic dynamic analysis of base-isolated buildings. After a review of basic theories and procedures of TELM, a typical shear-building model with and without seismic isolation is used to study the influence of seismic isolation on the seismic reliability of the structure. Two stochastic ground motion models, corresponding to “firm” and “soft” soil conditions, are considered to investigate the influence of soil condition on the effectiveness of seismic isolation. Crossing rates, first-passage probabilities, and fragility functions for the isolated and non-isolated structure, and for the two soil conditions are computed using TELM. Moreover, the computation of TELSs provides valuable insights into the mechanical properties of the seismically isolated structure.

2. Basics of the tail-equivalent linearization method

Consider a linear structural system subjected to a zero-mean, Gaussian stochastic seismic excitation $F(t)$ uniformly applied at all its supports. A generic response of the structure, $Z(t)$, can be expressed in terms of a Duhamel’s integral

$$Z(t) = \int_0^t h(t-\tau)F(\tau)d\,\tau, \tag{1}$$

in which $h(t)$ is a generalized IRF for the specific input-output pair. For TELM analysis, $F(t)$ is discretized and represented in terms of a finite set of random variables as

$$F(t) = \sum_{n=1}^{N} \mathrm{s}_n(t)\mathrm{u}_n = \mathbf{s}(t)\mathbf{u}, \tag{2}$$

where $\mathbf{u} = [u_1 \cdots u_N]^T$ is an n-vector of independent standard normal random variables, $\mathbf{s}(t) = [\mathrm{s}_1(t) \cdots \mathrm{s}_N(t)]$ is a row vector of deterministic basis functions dependent on the specific stochastic excitation model, and N is the number of terms used in the discrete representation. Substituting Eq. (2) in Eq. (1), one obtains

$$Z(t, \mathbf{u}) = \int_0^t h(t-\tau)\mathbf{s}(t)\mathbf{u}d\tau = \mathbf{a}(t)\mathbf{u}, \tag{3}$$

in which $\mathbf{a}(t) = [a_1(t) \cdots a_N(t)]$ and

$$a_n(t) = \int_0^t h(t-\tau)\mathrm{s}_n(t)d\tau, n = 1, \ldots, N \tag{4}$$

Note that $Z(t)$ is replaced by $Z(t, \mathbf{u})$ to explicitly indicate its dependence on random variables $\mathbf{u}$. Also note that vector $\mathbf{a}(t)$ contains the information about the IRF as well as the basis functions $s_n(t)$ that define the ground motion representation.

In the space of $\mathbf{u}$, define the limit-state function

$$G(\mathbf{u}, t, z) = z - Z(t, \mathbf{u}), \tag{5}$$

where z is a prescribed threshold for the response $Z(t, \mathbf{u})$ at time t. Note that $\Pr[G(\mathbf{u}, t, z) \leq 0] = \Pr[z \leq Z(t, \mathbf{u})]$ for varying z defines the complimentary cumulative distribution function (CCDF) of the response at time t. Let $\mathbf{u}^*(t)$ denote the *design point* in the context of the first-order reliability method (FORM) [14,15], i.e.,

$$\mathbf{u}^* = \arg\min\{\|\mathbf{u}\| \,|G(\mathbf{u}, t, z) = 0\} \tag{6}$$

In most cases, the design point $\mathbf{u}^*$ is computed using gradient based algorithms [16-18]. Using Eq. (3) and Eq. (6) in Eq. (5), one can easily show that [9]

$$\mathbf{a}(t) = z\frac{\mathbf{u}^{*\mathrm{T}}(t)}{\|\mathbf{u}^*(t)\|^2} \tag{7}$$

Note that $\mathbf{a}(t)$ is the gradient vector of the limit-state hyper-plane $G(\mathbf{u}, t, z) = z - \mathbf{a}(t)\mathbf{u} = 0$.

Next consider a nonlinear structure subjected to the discretized excitation in Eq. (2). Then, the generic response $Z(t, \mathbf{u})$ is a nonlinear function of $\mathbf{u}$. In TELM, the design point of the nonlinear system is used to define a hyperplane named TELS. This is equivalent of linearizing the limit state function at the design point. To completely identify the TELS in terms of its IRF, first the design point $\mathbf{u}^*$ of the nonlinear system is used in Eq. (7) to determine the gradient vector $\mathbf{a}(t)$; then, this is used in Eq. (4) to numerically solve for the IRF $h(t)$. The TELS is an equivalent system in the sense that the failure probability of the TELS is identical to the FORM approximation of the failure probability of the nonlinear system. Furthermore, the tangent hyper-plane of the nonlinear system response at the design point coincides with the hyper-plane of the linear system response for the same threshold and time.

The difference between time- and frequency- domain TELMs lies in the specific expression of $\mathbf{s}(t)$ in Eq. (2) and the way Eq. (4) is solved. In the time-domain TELM, the IRF in Eq. (4) is discretized at N time points, so that

$$\sum_{m=1}^{N} h(t-t_m)s_n(t_m)\Delta t \cong a_n(t), n, m = 1, \ldots, N, \tag{8}$$

where $t = t_N$, $t_m = m\Delta t$, and Δt is an incremental time step. The IRF is obtained by solving Eq. (8) for $h(t_N - t_m)$ at time points $t_N - t_1$, $t_N - t_2$,…, $t_N - t_{N-1}$.

For the frequency-domain TELM, the stationary stochastic excitation $F(t)$ is written in the form [19]

$$F(t) = \sum_{k=1}^{K/2} \sigma(\omega_k)[u_k \cos(\omega_k t) + u_{K/2+k} \sin(\omega_k t)], \tag{9}$$

where K is even, ω_k is a sequence of equally spaced frequency points with $\Delta\omega$ an incremental frequency step, (i.e., $\omega_k = \omega_{k-1} + \Delta\omega$, $k = 1, \ldots, K/2$, with $\omega_0 = 0$ and $\omega_{K/2}$ being the cut-off frequency of the process), $\sigma(\omega_k) = \sqrt{2S(\omega_k)\Delta\omega}$, and $S(\omega)$ is the two-sided power spectral density (PSD) of the process $F(t)$. Note that Eq. (9) is of the same form as the generalized Eq. (2) with index k (to underlie the frequency domain discretization) instead of n, and $s_k(t) = \sigma(\omega_k)\cos(\omega_k t)$ for $k = 1, \ldots, K/2$ and $s_k(t) = \sigma(\omega_k)\sin(\omega_k t)$ for $k = K/2 + 1, \ldots, K$. Using the frequency-domain representation Eq. (9) and basic principles of frequency-domain analysis [10], Eq. (4) leads to

$$\begin{aligned} a_k(t) &= \sigma(\omega_k)|H(\omega_k)|\cos(\omega_k t + \varphi_k) \quad \text{for } k = 1, \ldots, K/2 \\ &= \sigma(\omega_k)|H(\omega_k)|\sin(\omega_k t + \varphi_k) \quad \text{for } k = K/2 + 1, \ldots, K, \end{aligned} \tag{10}$$

where $|H(\omega)|$ is the modulus of the FRF, φ is the phase angle of the FRF, and $a_k(t)$ are obtained from Eq. (7). The modulus and phase angle of the FRF are easily computed from Eq. (10).

With the IRF/FRF obtained from time/frequency domain TELM analysis, various response statistics can be effortlessly computed using linear stochastic dynamics.

To conclude, the procedures of TELM analysis can be generalized as follows.

I. Discretize the ground motion into a finite set of random variables. Time or frequency domain discretization are both equally valid options (see [19, 20]).

II. For a specified threshold z, compute the design point $\mathbf{u}^*$ using optimization algorithms (see [16, 17]).

III. Compute the gradient vector of TELS using Eq. (7).

IV. Solve for the IRF using Eq. (4) (time domain), or for the FRF using Eq. (10) (frequency domain).

V. Compute response statistics such as the crossing rates, first-passage probability, fragility functions using standard linear stochastic dynamics (see [9]).

The procedures II-V are often repeated for a sequence of thresholds, so that response distributions can be numerically obtained. It is important to note that TELS will vary as the threshold z in procedure II varies, unless the structure is linear. This property allows TELM to capture the non-Gaussianity of the nonlinear response.

TELM is remarkably efficient for computing fragility functions, i.e.

$$\mathrm{Fr}(s) = \Pr[G(\mathbf{u}, \mathrm{S}) \le 0 | S = s], \tag{11}$$

where s is a scaling factor of the ground motion, and $G(\mathbf{u}, \mathrm{S})$ is the performance function. It can be shown that TELS is independent of the scaling of the ground motion [9], so that the same TELS can be used to estimate the fragility function.

3. TELM analysis of base-isolated building model

3.1 Analysis model

Consider a 6-DOF base-isolated shear-building model shown in Fig. 1. We assume a rubber bearing isolation system for which the force-deformation behavior can be expressed as a one-dimensional non-degrading Bouc-Wen model [21] i.e.

$$\begin{aligned} k[\alpha X(t) + (1-\alpha)Z(t)] &= F_k(t) \\ \dot{Z}(t) = -\gamma\big|\dot{X}(t)\big||Z(t)|^{\bar{n}-1}Z(t) &- \eta|Z(t)|^{\bar{n}}\dot{X}(t) + A\dot{X}(t), \end{aligned} \tag{12}$$

where parameters of the Bouc-Wen model are set as: $k = 0.2 \times 10^4$[kN/m], $\alpha = 0.05$, $\bar{n} = 3$, $A = 1$ and $\gamma = \eta = 1/(2u_y^{\bar{n}})$, in which $u_y = 0.01$[m]. The superstructure is assumed to be linear. The based-isolated structure has an initial fundamental period of 1.933[sec] and second mode period of 0.312[sec]. The corresponding non-isolated structure (the superstructure of the isolated model) has an initial fundamental period of 0.511[sec] and second mode period of 0.215[sec]. The damping ratio for the bearing is set to 20%, and the damping ratio for each mode of the superstructure is set to 5%. The structure is subjected to a stochastic ground motion with a duration of 10[sec]. The acceleration power spectrum density (PSD) of the ground motion is described by a modified Kanai-Tajimi model suggested by Clough and Penzien [22]

$$S(\omega) = S_0 \frac{\omega_f^4 + 4\zeta_f^2\omega_f^2\omega^2}{(\omega_f^2 - \omega^2)^2 + 4\zeta_f^2\omega_f^2\omega^2} \frac{1}{(\omega_g^2 - \omega^2)^2 + 4\zeta_g^2\omega_g^2\omega^2}, \tag{13}$$

where S_0 is a scale factor, ω_f and ζ_f are the filter parameters representing, respectively, the natural frequency and damping ratio of the soil layer, and ω_g and ζ_g are parameters of a high pass filter introduced to assure finite variance of the ground displacement. Two soil conditions associated with “firm” and “soft” soils are considered with the parameter values listed in Table 1. The scale factors S_0 in Table 1 are selected such that the mean peak ground acceleration of the stochastic ground motions for the two soil conditions are around 0.5g.

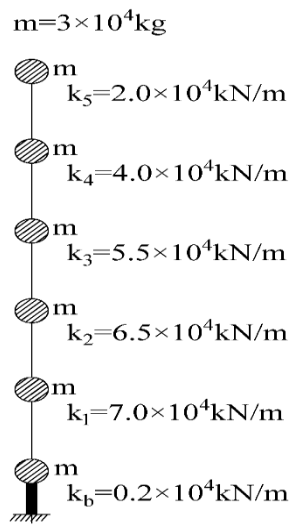

Fig. 1 – Structure model

Table 1 – PSD parameters for model soil types

Soil type	S_0 [m^2/s^3]	ω_{fk} [rad/s]	ζ_{fk}	ω_{gk} [rad/s]	ζ_{gk}
Firm	0.031	15.0	0.6	1.5	0.6
Soft	0.082	5.0	0.2	0.5	0.6

The acceleration PSDs for the two soil conditions are illustrated in Fig. 2.

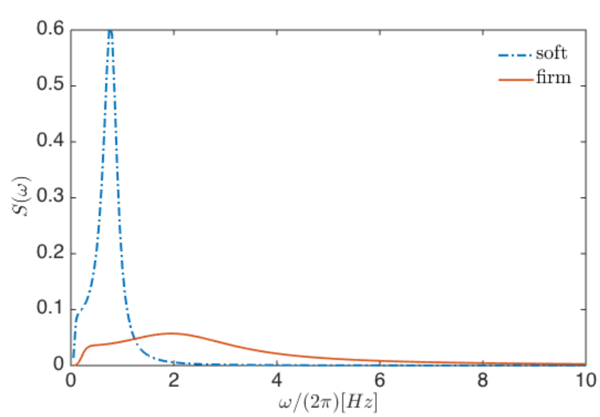

Fig. 2 –PSDs of ground acceleration for two soil conditions

Using the ground acceleration PSD models, the ground motion processes can be discretized into a finite set of random variables. In this paper, the frequency domain discretization is used (see Eq. (9)). The cut-off frequency is set to $20\pi[\mathrm{rad/s}]$ (10 [Hz]), and the frequency step $\Delta\omega$ is set to $0.1\pi[\mathrm{rad/s}]$. The number of random variables is 400.

3.2 Design point excitations and responses

In structural reliability theory, the design point is the point belonging to the failure domain with the highest probability density function. In stochastic dynamic analysis via TELM, the design point defines the so-named design-point excitation, which is the realization belonging to the failure domain with the highest probability density. The structural response arising from the design-input excitation is the so-named design-point response. The drift of the top floor (5^{th} floor for the superstructure) is considered as the response quantity of interest. A threshold $z = 0.01[\mathrm{m}]$ and time point $t_n = 10[\mathrm{sec}]$ are considered to illustrate the design point, design point excitations and responses. Fig. 3 shows the design point excitations and responses for the two structures and the two ground motion models. Also, the reliability indexes are listed in Fig. 3. In Fig. 3, points from u=1 to u=200 are associated with the u_p component in Eq. (9), and points from u=201 to u=400 are associated with the $u_{K/2+k}$ component in Eq. (9)

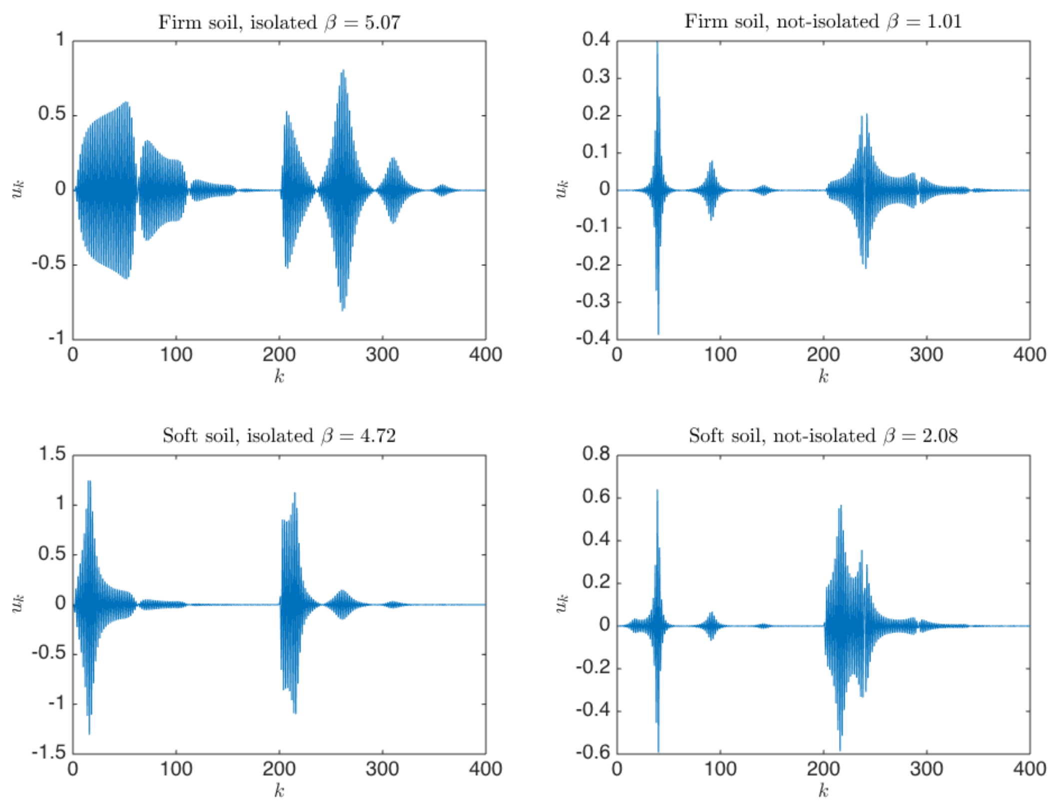

Fig. 3 –Design points for different structures and soil models

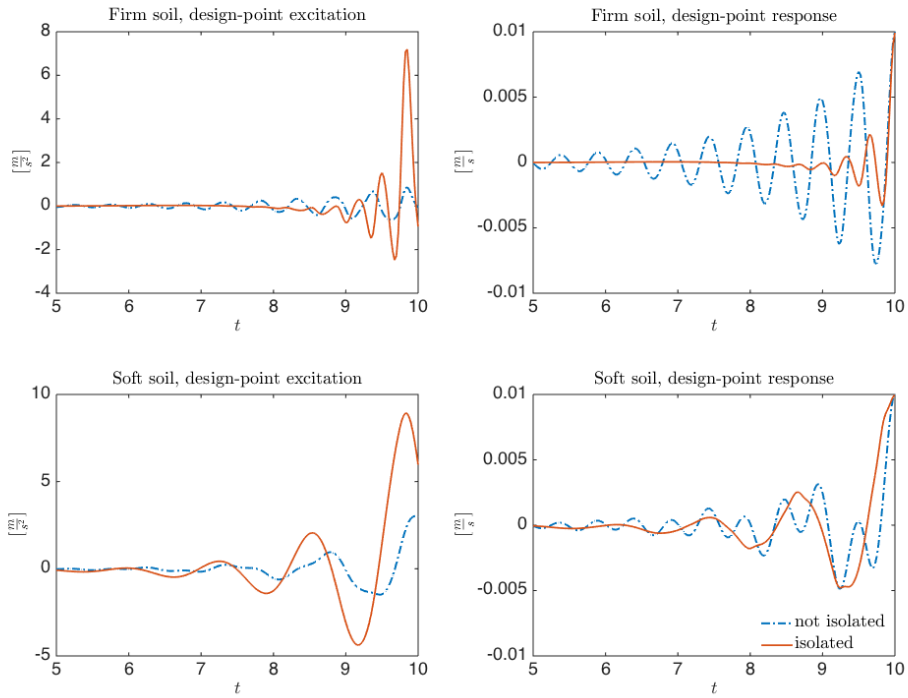

Fig. 4 –Design point excitations and responses for different structure and soil models

The following observations in Fig. 3 and Fig. 4 are noteworthy:

I. For both of the soil conditions, the design points for the isolated structure model have a richer low frequency content than the non-isolated one. Consequently, the design point excitations and responses for the isolated model show less oscillations than the non-isolated one, since the energy is driven into the system from the bearing period.

II. For both isolated and non-isolated models, lower frequency contents of the design point for soft soil condition are more significant than that for firm soil condition. As a result, the design point excitations and responses for the soft soil condition exhibit less oscillations than the firm soil condition.

III. For both of the soil conditions, the use of base-isolation significantly increases the reliability indexes for the given thresholds.

IV. Given the assigned parameters, the reliability index for the firm soil condition is smaller than the reliability index for the soft soil condition; however, an opposite behavior is observed for the isolated model. This suggests that the presence of soft subsoil could decrease the effectiveness of base isolation. Further studies with different soil periods needs to be developed before drawing additional conclusions.

3.3 Frequency-response functions of the tail-equivalent linear system

The frequency-response functions (FRFs) of the tail-equivalent linear system for the two different structures, the two soil models, and for different threshold values are illustrated in Fig. 5. The FRFs shown in Fig. 5 characterize the amplitude of harmonic drift of the top floor for a harmonic ground acceleration.

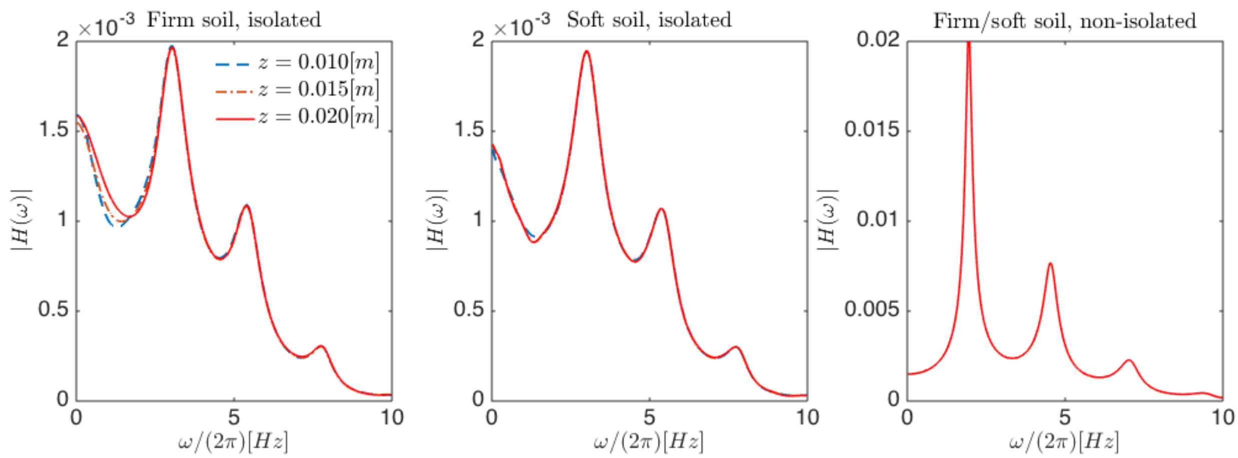

Fig. 5 –Frequency response functions for different structures and thresholds

Note that since the superstructure is linear, the FRF of the non-isolated model is a physical property that is independent of the threshold or subsoil condition. As expected, the FRF of the isolated model has richer low frequency content, and its amplitude is much smaller than that of the non-isolated model. Observe that the FRF of the isolated model is not overly sensitive to the threshold. This is the result of the current assumptions. In particular, the bearing system yields rapidly and essentially acts like a linear system with stiffness equal to its post hardening stiffness. Since this is considerably softer than the initial stiffness, the mode spacing (between bearing period and superstructure period) is enlarged. Consequently, the bearing system acts as a linear filter in series. As result, the response of the superstructure can be interpreted as the response of a linear system to a color noise. The color noise is defined by the combination of the input PSD and the PSD of the isolator filter. Given this interpretation, it follows that the TELS is invariant to the threshold. However, different assumptions may lead to different conclusions.

3.4 Response statistics

Crossing rates, first-passage probability distributions, and the fragility functions with respect to the mean peak ground acceleration and the first-passage probability of the top-floor drift at threshold $z = 0.01$[m] for different structure and soil models are illustrated in Fig. 6. Results of Fig. 6 are computed using linear random vibration solutions.

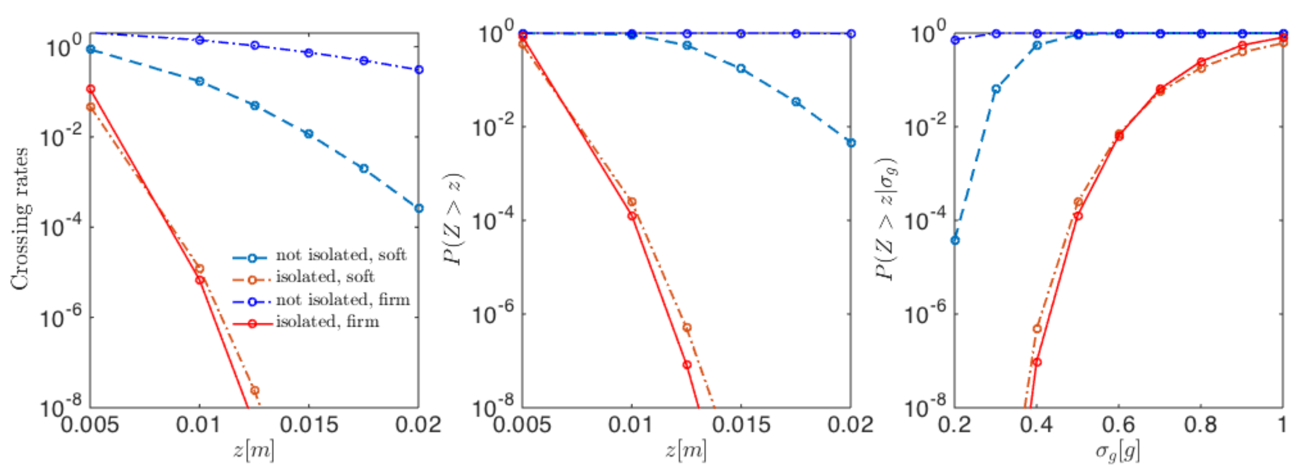

Fig. 6 –Crossing rates, first-passage probabilities and fragility functions for different structural and soil models

Fig. 6 implies similar mechanical properties of the base-isolated structure as described in the previous two subsections.

Finally, as discussed in the previous subsection, given the assumption underlying this study, the FRF of TELS seems not sensitive to the threshold, thus it might be valid to only compute one design point and the corresponding FRF in determining response statistics. Fig. 7 corroborates this idea. The figure shows the first-passage probability distributions of the top-floor drift obtained from the TELM analysis using a sequence of design points compared with the result obtained from using only one design point for threshold $z = 0.01[\mathrm{m}]$. Note that the result illustrated in Fig. 7 is associated with the firm soil condition. It is found that for soft soil condition and other response statistics, the trend in Fig 7 still holds.

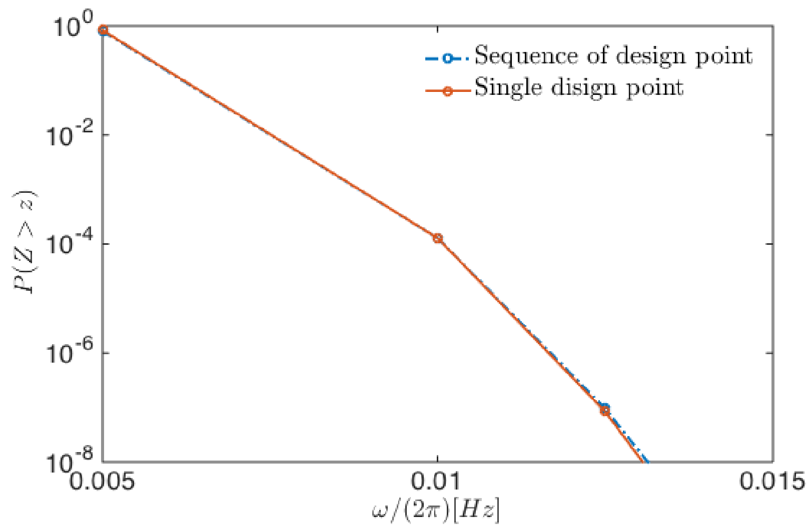

Fig. 7 –First-passage probability distribution estimations from TELM using a sequence and single design points

4. Conclusions

The paper studies stochastic dynamic behavior of base-isolated buildings using tail-equivalent linearization method (TELM). A base-isolated shear-building model and the corresponding non-isolated model are studied. Two soil conditions associated with firm and soft subsoils are considered. Response statistics such as the crossing rate, first-passage probability distribution and fragility function are computed using linear random vibration solutions for the tail-equivalent linear system (TELS). It is found that the presence of base-isolation bearing significantly increases the reliability of the structure, although the base-isolation tends to be less effective for soft subsoil condition. For this example, it is also found that TELS is not overly sensitive to the response thresholds when the superstructure is considered elastic. Given this, it is reasonable to compute only one design point to obtain the response statistics.

5. Acknowledgements

The first and second author are supported by the Program for Changjiang Scholars and Innovative Research Team for the research group of Prof. Zhishan Li at Guangzhou University (Grant No. IRT13057), and by the National Science and Technology Major Project of the Ministry of Science and Technology of China (Grant No. 2016YFB0200605). This support is gratefully acknowledged.

6. References

[1] Caughey TK (1963). Equivalent linearization techniques. *Journal of the Acoustical Society of America*, **35**:1706-1711.

[2] Atalik TS, Utku S (1976). Stochastic linearization of multi-degree of freedom nonlinear systems. *Earthquake Engineering and Structural Dynamics*, **4**: 411-420.

[3] Roberts JB, Spanos PD (2003). *Random vibration and statistical linearization*, Courier Dover Publications, Mineola, NY.

[4] Wen YK (1980). Equivalent linearization for hysteretic systems under random excitation. *Journal of Applied Mechanics (ASME)*, **47**:150–154.

[5] Ates S, Dumanoglu A, Bayraktar A (2005). Stochastic response of seismically isolated highway bridges with friction pendulum systems to spatially varying earthquake ground motions. *Engineering Structures*, **27**:1843–1858.

[6] Jangid RS (2008). Stochastic response of bridges seismically isolated by friction pendulum system. *Journal of Bridge Engineering*, **13**(4):319–330.

[7] Curadelli O (2013). Equivalent linear stochastic seismic analysis of cylindrical base-isolated liquid storage tanks. *Journal of Constructional Steel Research*, **83**:166–176.

[8] Greco R, Marano GC, Mezzina M (2001). The performance of HDRB devices in base isolation: A stochastic sensitivity analysis. *Journal of Structural Control*, **8**:203–218.

[9] Fujimura K, Der Kiureghian A (2007). Tail-equivalent linearization method for nonlinear random vibration. *Probabilistic Engineering Mechanics*, **22**:63-76.

[10] Garre L, Der Kiureghian A (2010). Tail-equivalent linearization method in frequency domain and application to marine structures. *Marine Structures*, **23**: 322-338.

[11] Broccardo M (2014). Further development of the tail-equivalent linearization method for nonlinear stochastic dynamics. *Ph.D Thesis*, University of California, Berkeley.

[12] Broccardo M, Der Kiureghian A (2015). Multicomponent nonlinear stochastic dynamic analysis by tail-equivalent linearization. *Journal of Engineering Mechanics*, 04015100.

[13] Wang Z, Der Kiureghian A (2016). Tail-equivalent linearization of inelastic multi-support structures subjected to spatially varying stochastic ground motion. *Journal of Engineering Mechanics*. 04016053.

[14] Ditlevsen O, Madsen HO (1999). *Structural reliability methods*. Wiley.

[15] Der Kiureghian A (2005). First- and second-order reliability methods. In: E. Nikolaidis, D.M. Ghi-ocel, S. Singhal (Eds.), *Engineering design reliability handbook*. Boca Raton (FL): CRC Press.

[16] Liu PL, Der Kiureghian A (1991). Optimization algorithms for structural reliability. *Structural Safety*, **9**(3):161-177.

[17] Haukaas T, Der Kiureghian A (2006). Strategies for finding the design point in non-linear finite element reliability analysis. *Probabilistic Engineering Mechanics*, **21**:133-147.

[18] Wang Z, Broccardo M, Der Kiureghian A (2016). An algorithm for finding a sequence of design points in reliability analysis. *Structural Safety*, **58**:52-59.

[19] Shinozuka M, Deodatis G (1991). Simulation of stochastic processes by spectral representation. *Applied Mechanics Reviews*, **25**: 191-204.

[20] Rezaeian S, Der Kiureghian A (2008). A stochastic ground motion model with separable temporal and spectral nonstationarities. *Earthquake Engineering and Structural Dynamics*, **37**(13): 1565–1584.

[21] Bouc R (1963). Forced vibration of mechanical systems with hysteresis. *Proceeding of Fourth Conference on Nonlinear Oscillation*. Academia Publishing: Prague, Czechoslovakia, 315.

[22] Clough RW, Penzien J (1975). *Dynamic of structures*, McGraw-Hill, New York.